KONA Powder and Particle Journal

KONA Powder and Particle Journal No. 43 (2026) 47–62/https://doi.org/10.14356/kona.2026012 Review Paper

Specific Ion Effects in the Handling of Particle Suspensions: A Review †

Tomonori Fukasawa

Chemical Engineering Program, Graduate School of Advanced Science and Engineering, Hiroshima University, Japan

Specific ion effects (SIEs) play a pivotal role in governing particle suspension behavior and manipulation across diverse scientific and industrial fields. This review summarizes the underlying mechanisms of SIEs, focusing on ion accumulation at particle interfaces, Hofmeister series implications, electrokinetic properties, and their impact on coagulation, dispersion, and rheological characteristics. It examines the interplay among ion identity, concentration, and surface properties—including hydrophilicity, hydrophobicity, and surface-charge density—offering critical insights into particle–particle interactions. Particular emphasis is placed on the structural and electrostatic roles of the electrical double layer and the Stern layer. Recent advances in understanding the microscopic origins of SIEs, facilitated by innovative experimental approaches and computational modeling, are also highlighted. This review explores the influence of SIEs on aggregate formation and stability, gelation behavior, and suspension viscoelastic properties. These insights underscore the significance of accounting for SIEs across disciplines such as chemistry, industry, agriculture, environmental science, biology, and medical science, and emphasize the need for continued advances to realize innovative applications and transformative solutions.

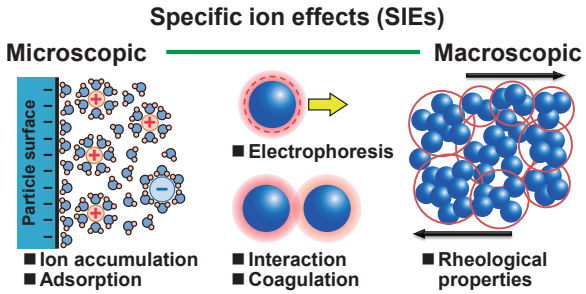

Keywords: specific ion effects, Hofmeister series, particle suspension, ion hydration, electrokinetic phenomena, rheology

1. Introduction

The presence of ions in a particle suspension profoundly affects its properties. Electrolytes, including acids, bases, and salts, are encountered in numerous fields across the chemical, industrial, agricultural, environmental, biological, and medical sciences. In these fields, electrolyte effects depend not only on the valence and concentration of ions, as suggested by the Debye–Hückel (DH) theory, but also on their identities. The effects of ions on system properties are collectively called specific ion effects (SIEs) (Mazzini and Craig, 2016). The DH theory addresses the electrostatic potential in an electrolyte solution by linearizing the Poisson–Boltzmann equation. It assumes that the ions are nonpolarizable point charges that fully dissociate in a uniform, featureless dielectric solvent. However, by neglecting ion-specific properties such as size, shape, polarizability, and charge density, the DH theory has limited applicability in explaining SIEs.

Franz Hofmeister's groundbreaking work (Hofmeister, 1888; Kunz et al., 2004a) is widely acknowledged as the first systematic study of SIEs. Consequently, SIEs are often referred to as Hofmeister effects. Hofmeister classified ions into sequences, now known as the Hofmeister series, based on their effects on protein solubility and denaturation. This classification has been consistently observed in numerous experimental systems (dos Santos et al., 2010; López-León et al., 2003; Zhang et al., 2005). Importantly, SIEs were not exclusively associated with water. Several research groups have explored this phenomenon in nonaqueous environments, where ion–solvent and solvent–solvent interactions (including dispersion forces) have been effectively used to explain SIEs (Freire et al., 2009; Labban and Marcus, 1991, 1997; Peruzzi et al., 2015).

Fig. 1 presents the extended Hofmeister series (HS) for anions and cations, with the shapes and bare radii of ions depicted approximately to scale, allowing identification of their properties (Bastos-González et al., 2016). In the Hofmeister effect studies, Na^+ and Cl^- are typically used as reference ions. The anions to the right of Cl^- are chaotropes, less hydrated and disrupting order in solution, while those to the left are kosmotropes, more hydrated and bringing order. Similarly, in cationic HS, cations left of Na^+ are chaotropes (less hydrated), and those to the right are kosmotropes (more hydrated). Kosmotropes precipitate (salt-out) proteins, while chaotropes solubilize (salt-in) proteins. However, despite their widespread historical use, the terms "kosmotrope" and "chaotrope" can be misleading when considering the relative standard molar entropies of various

† Received 31 January 2025; Accepted 26 March 2025
J-STAGE Advance published online 24 June 2025
Add: 1-4-1 Kagamiyama, Higashi-Hiroshima City, Hiroshima, 739-8527, Japan
E-mail: fukasawa@hiroshima-u.ac.jp
TEL:+81-82-424-7854 FAX: +81-82-424-7854

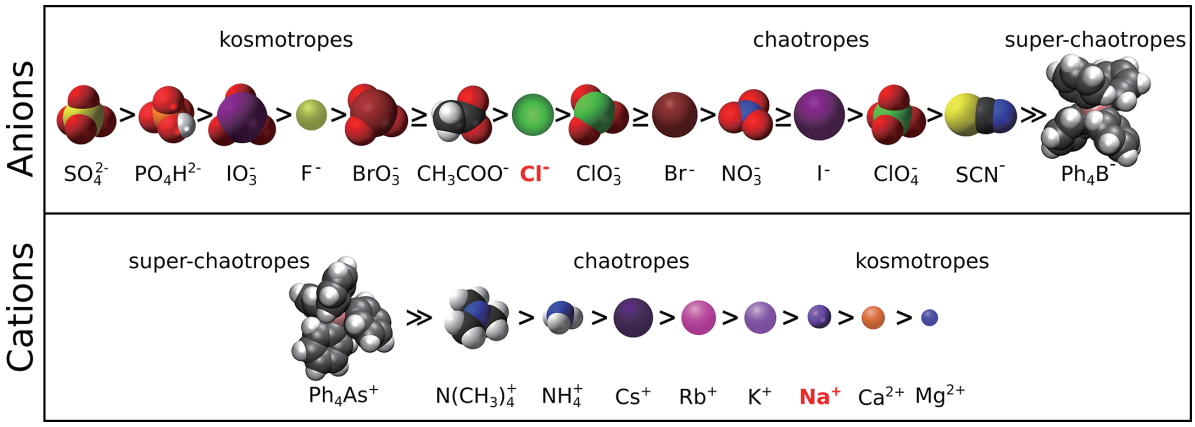

Fig. 1 Extended Hofmeister series (HS) of anions and cations. Tetraphenyl ions are included as super-chaotropes. Adapted with permission from Ref. (Bastos-González et al., 2016). Copyright: (2016) Elsevier B.V.

ions (Gregory et al., 2019). To address this, Gregory et al. (2022) suggested replacing these terms with "charge-diffuse ion" for chaotropes and "charge-dense ion" for kosmotropes. The Hofmeister sequences in **Fig. 1** are direct HS (HSs). These data were derived from studies on hen egg white protein precipitation at low pH, where the protein is positively charged. Here, anions act as counterions, and cations act as co-ions. When the protein is negatively charged (at basic pH), the roles of anions and cations as counterions and co-ions reverse, inverting the HS sequences (Boström et al., 2005); these reverse sequences are indirect HS.

The widespread presence of HS suggests that the ion properties play a fundamental role in their origin. Collins and Washabaugh (1985) initially identified 30 characteristics of salt solutions, a list that has since grown with traits like ion size, polarizability, and hydration free energy, partially aligned with Hofmeister trends (Gregory et al., 2021; Kunz et al., 2004b). However, variations and exceptions have prevented the establishment of clear Hofmeister parameters. Leontidis (2017) explored these properties and proposed that HS arises from a combination of ionic charge distribution, size, shape, and hydrophobicity.

Fig. 1 reveals the existence of a partial correlation between ion size and HS (Parsons and Ninham, 2009). Large symmetrical ions (e.g., I^-) possess delocalized and polarizable electron densities, making them less effective at forming orientation-dependent bonds, like hydrogen bonds. In contrast, small ions (e.g., F^-) exhibit high-charge densities, enabling strong directional interactions. Consequently, large ions typically possess weak solvation shells (Collins et al., 2007), which facilitate their desolvation and interaction with the cosolutes. The ion shape is another crucial factor because it can induce anisotropic charge densities (e.g., SCN^-), unlike in monatomic ions. Other critical characteristics influencing Hofmeister trends include ion polarizability, radial charge density, viscosity coefficients, solubility, ion pairing, and Lewis acidity/basicity. A previously reported extensive review provides comprehensive insights into these characteristics (Gregory et al., 2022).

HS can be reportedly reversed, or certain ions may appear at positions different from those in the original HS, depending on the characteristics of the surface of interest (Lyklema, 2009; Zhang and Cremer, 2009). Thus, discussing the universal characteristics of HS is challenging. However, in many cases, HS inversion or sequence variation can be explained by considering the surface's hydrophobic/hydrophilic properties and charge sign. For example, the aggregation behavior of negatively charged colloids aligns with the usual direct HS, whereas positively charged colloids exhibit an inverse sequence. Another reversal is observed when the particle surface properties shift from hydrophobic to hydrophilic (López-León et al., 2003, 2008). HS reversal due to pH changes has also been observed for surfaces with dissociable functional groups (Dumont et al., 1990; Lyklema, 2003, 2009; Morag et al., 2013; Schwierz et al., 2015).

This review focuses on SIEs, including HS, emphasizing the phenomena encountered in the handling of particle suspensions, such as ion accumulation on the particle surface, electrokinetic phenomena of particles, and the coagulation, dispersion, and rheological properties of particle suspensions.

2. SIEs at particle interfaces

Understanding and predicting ion behavior at particle interfaces—the most fundamental aspects at the microscopic level—is crucial for the effective control and manipulation of particle suspensions. This article provides an overview of the impact of ion hydration, ion concentration, hydrophilic or hydrophobic nature, and signs of charge density of particle surfaces on the ion behavior at particle interfaces. Furthermore, this study highlights the impact of SIEs on the electrical double layer (EDL) and Stern layer formed around the particle interfaces.

2.1 Hydrophilic and hydrophobic characteristics of ions and particle surfaces

Levin and Santos (2014) proposed a theory suggesting that chaotropic anions tend to accumulate on hydrophobic colloids, whereas kosmotropic anions are excluded from surfaces. They indicated that chaotropic anions lose their hydration shells when interacting with hydrophobic interfaces, which plays a key role in determining the polarizability and bare radii of the anion. Conversely, the high electrostatic solvation energy of kosmotropic anions prevents their adsorption onto hydrophobic interfaces, ensuring that they remain hydrated. In this context, the critical parameter is the hydrated radius of the anions. The proposed theory is closely supported by experimental data on the interfacial tension excess at the air–water interface and the colloidal stability of polystyrene particles.

Schwierz et al. (2010, 2013, 2015, 2016) reported detailed insights into the distribution of anions and cations at the solid–water interface of surfaces with various functional groups using molecular dynamics simulations. **Table 1** summarizes the surface affinities of halide anions and alkali cations on surfaces terminated with hydrophobic methyl (CH_3), polar hydroxide (OH), polar carboxyl (COOH), and charged carboxylate (COO^-) groups. The anions showed a clear reversal in binding affinity when compared with hydrophobic and hydrophilic surfaces. This situation is more complex for cations with a mix of direct, reversed, and partially altered series. To understand microscopic surface affinity, discussing ion–surface interactions on hydrophobic surfaces (CH_3-terminated) and hydrophilic (polar) surfaces (OH-terminated) is essential. The surface affinity of single ions can be quantified by calculating the free-energy profile (the potential of the mean force, PMF) (**Fig. 2A and B**). On hydrophobic surfaces, the affinity is proportional to the ion size, with larger ions (e.g., Cs^+ and I^-) exhibiting the strongest adsorption, whereas the affinity decreases as the ion size becomes smaller. The high affinity of large ions can be explained by hydrophobic solvation theory (Huang et al., 2008; Schwierz et al., 2013). In contrast, Li^+ exhibits unique behavior as it retains its primary hydration shell, irrespective of its distance from the surface (Schwierz et al., 2013). Large ions shed hydration water molecules and preferentially adsorbed onto the hydrophobic surface (**Fig. 2C**), whereas smaller ions tended to retain their hydration shells and were more likely to be repelled from the hydrophobic interface. On hydrophilic OH-terminated surfaces, the affinity of anions is reversed, with smaller ions, such as F^-, being less repelled and preferentially adsorbed. This phenomenon arises from the strong interactions between the anions and hydrogen atoms of the OH groups, which possess a high surface-charge density (Collins, 1997). Specifically, anions preferentially interact with these high-charge-density hydrogen atoms, allowing small ions like F^- to adsorb easily and form contact pairs with several surface hydrogen atoms simultaneously. In contrast, small cations are more inclined to interact with oxygen atoms, which possess a moderate surface-charge density, with Li^+ showing the strongest surface affinity and K^+ the weakest. Cs^+ interacts favorably at large surface separations, exhibiting partially reversed behavior. The adsorption or exclusion of ions at surfaces is governed by direct ion–surface interactions, delicate balance of ion hydration in bulk solutions, and energetic costs associated with partial ion dehydration during surface binding.

Table 1 Summarizes the ion-specific affinities of surfaces with different functional groups: hydrophobic methyl (CH_3), polar hydroxide (OH), polar carboxyl (COOH), and charged carboxylate (COO^-) groups. The ranking shows the ordering of anions and cations according to their surface binding affinities, derived from single-ion free-energy profiles and interfacial tensions (Schwierz et al., 2010, 2013, 2015, 2016). Adapted with permission from Ref. (Schwierz et al., 2016). Copyright: (2016) Elsevier B.V.

Functional group	Anion binding affinity	Cation binding affinity
CH_3	$I^- > Cl^- > F^-$	$Cs^+ > Li^+ > K^+ > Na^+$
OH	$F^- > Cl^- > I^-$	$Li^+ > Cs^+ > Na^+ > K^+$
COOH	$F^- > Cl^- > I^-$	$Cs^+ > Na^+ > Li^+$
COO^-	$F^- \geq Cl^- \geq I^-$	$Li^+ > Na^+ > Cs^+$

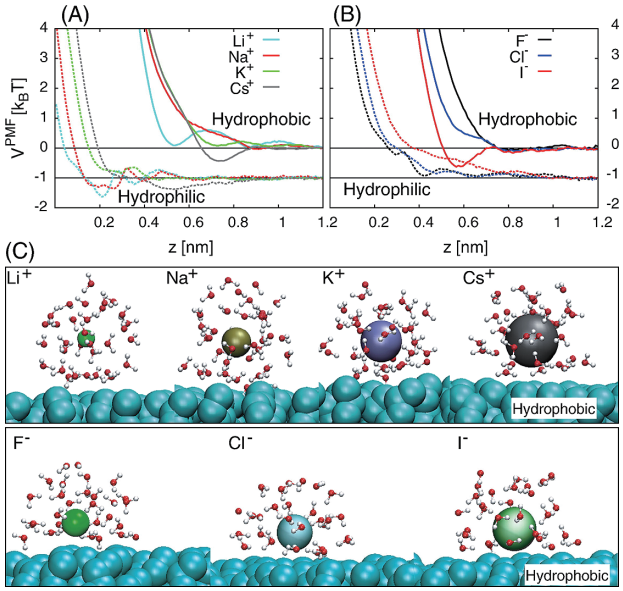

Fig. 2 Free energy profiles for cations **(A)** and anions **(B)** at the hydrophobic surface (solid lines) and the hydrophilic surface (dotted lines) depending on the ion–surface separation z. The PMFs at the hydrophilic surface are shifted vertically for clarity. **(C)** Simulation snapshots at the hydrophobic surface. Top: cations at $z = 0.75$ nm (minimum in the PMF of Cs^+). Bottom: anions at $z = 0.575$ nm (minimum in the PMF of I^-). Water molecules within 6 Å of the ions are shown, and their ionic sizes correspond to their Pauling radii. Extended Hofmeister series of anions and cations is also shown, with tetraphenyl ions included as super-chaotropes. Adapted with permission from Ref. (Schwierz et al., 2016). Copyright: (2016) Elsevier B.V.

2.2 Signs of the particle surface charge and ion concentration

The surface-charge density sign has a significant impact on the HS. On negatively charged surfaces, strongly adsorbing cations efficiently compensate for the surface charge, resulting in minimal stabilization for large cations (e.g., Cs^+) (direct series). Conversely, on positively charged surfaces, specific cation adsorption increases the surface charge, leading to the maximum electrostatic stabilization by large cations (indirect series). For anions, the picture is opposite: on negatively charged surfaces, large anions (e.g., I^-) further increase the surface charge (direct series), whereas on positively charged surfaces, large anions effectively compensate for the surface charge (indirect series). In addition, a salt concentration-dependent HS reversal was observed. At low salt concentrations, a series of positively charged solutes (particles) followed an indirect order. However, at high salt concentrations, counterion adsorption overcompensated for the positive charge, resulting in effectively negative surfaces in the KCl and NaCl solutions. In contrast, in the CsCl solutions, the positive charge was maintained but reduced in magnitude, leading to the reappearance of the direct series at high salt concentrations. Schwierz et al. (2016) summarized these results in a phase diagram of cationic HS as a function of surface-charge density and salt concentration, displaying the complete spectrum of direct, partially altered, and fully reversed HS.

2.3 The pH value of the dispersion medium

The acidic surface groups of oxides and proteins undergo protonation or deprotonation depending on their pH, leading to changes in their surface charge and chemical structure. These changes modify the interactions between the surrounding ions and the hydration water, directly influencing ion-specific adsorption. A notable example is the reversal in the cation-binding affinities between the uncharged carboxyl (COOH) and charged carboxylate (COO^-) surface groups (**Table 1**). At low pH, the carboxyl surface is protonated and thus charge neutral, favoring the adsorption of large cations (e.g., Cs^+). In contrast, at high pH, carboxyl groups are deprotonated (COO^-), and small cations (e.g., Li^+ and Na^+) exhibit higher affinity, leading to the observation of the reversed series.

The stabilization of surfaces containing acidic groups occurs via deprotonation and ion-specific adsorption. pH-dependent HS reversal is a characteristic of acidic surfaces. At low pH, the absolute value of the surface charge is small, and the series follows direct HS, with reversal occurring near-neutral pH (Morag et al., 2013). This reversal from the direct HS at low pH to the reversed series at high pH was attributed to the inversion of cation-binding affinities between the protonated (low pH) and deprotonated (high pH) acidic groups (Schwierz et al., 2015).

A Hofmeister phase diagram summarizing the efficiency of different cations in stabilizing surfaces containing acidic surface groups as a function of pH and salt concentration has been proposed (Schwierz et al., 2016). At an intermediate pH, the direct series dominated, whereas at a high pH, the reversal of cation affinities for protonated and deprotonated acidic groups explained the observed behavior. For instance, at high pH, small Li^+ ions show higher affinity for carboxylate groups, resulting in stronger stabilization compared to Cs^+. For intermediate pH, Cs^+ binds most strongly to neutral carboxyl groups and compensates for the negative charge of acidic surface groups more efficiently, which aligns with direct HS. At a low pH, the increased adsorption of Cs^+ leads to the reversal of the effective surface charge, causing additional changes in the HS (Schwierz et al., 2015). In contrast, for the anions, the binding affinity did not significantly change with the deprotonation of the carboxyl groups. Consequently, the HS of the anions remained largely unaffected by pH changes (see **Table 1**).

2.4 Electrical double layer and Stern layer

When a solid surface comes into contact with an aqueous solution, excess positive or negative charges are generated, leading to the rearrangement of ions in the adjacent electrolyte to shield the charges and form an EDL (Lyklema, 1995; Morag et al., 2013; Siretanu et al., 2014). The EDL plays a fundamental role in controlling surface structures (Nihonyanagi et al., 2010; Toney et al., 1994), regulating interfacial reactivity (Bunton et al., 1991), interactions between particles, and mitigating interactions between drug carriers and cells (Jiang et al., 2015). The potential of a solid surface with an EDL generally exceeds the electrokinetic potential, and this difference is often substantial. To account for this discrepancy, a Stern layer composed of non-specifically adsorbed ions has been traditionally proposed. The thickness and potential of the Stern layer are significantly influenced by SIEs; however, their quantitative evaluation is challenging.

Brown et al. (2016) used X-ray photoelectron spectroscopy (XPS) from a liquid microjet to measure the absolute surface potential of silica nanoparticles in aqueous solutions. They investigated the effects of specific cations (Li^+, Na^+, K^+, and Cs^+) in chloride electrolytes on the surface potential, shear plane position, and Stern layer electrostatic capacitance. Their findings showed a linear relationship between surface potential magnitude and hydrated cation radius, which was attributed to increased cation distance from the surface, causing a larger potential drop across the Stern layer. These results suggest that the microscopic origin of the specific ion effect lies in the larger electrostatic capacitance caused by the smaller hydrated cations approaching the Stern layer. Furthermore, the thickness of the Stern layer corresponds to the sum of the monolayer of water molecules hydrating the silica surface and the radius of the hydrated cation (**Fig. 3**). These findings closely align

with atomic force microscopy (AFM) imaging results, which directly visualize the ions within the Stern layer (Siretanu et al., 2014). Additionally, the Stern layer thickness predicted at the limit of the zero-cation radius corresponds to a monolayer of water molecules on the oxide surface, providing intuitive validation of the model. By employing a hydration-modified Poisson–Boltzmann model that includes soft non-electrostatic interactions to describe the hydration repulsion between counterions, the authors successfully reproduced SIEs quantitatively. This was achieved using only the measured surface-charge density and hydrated cation radius as input parameters.

Vibrational sum-frequency generation (vSFG) spectroscopy was used to distinguish different populations of water molecules within the EDL at the silica–water interface (Darlington et al., 2017). Through a systematic analysis of the variations in the electrolyte concentration (10–100 mM NaCl), pH (surface deprotonation), and SFG polarization combinations, two pH-dependent water molecule regions were established: one located near the surface within the Stern layer and the other located further from the surface in the diffuse part of the EDL. Most strikingly, the orienting forces influencing different populations of water molecules exhibited significant variations with changes in pH at high salt concentrations. In the case of water molecules adjacent to the surface within the Stern layer, an increase in the pH from the point of zero charge (PZC) of silica (approximately pH 2) to higher levels led to enhanced alignment, reflecting the increasingly negative charge of the surface. In contrast, water molecules located farther from the surface exhibited a net flip in orientation upon increasing the pH over the same range. These findings suggest the presence of oriented water near the PZC (under low pH conditions). This oriented water is due to water being oriented farther from the surface, influenced by either interactions with cations at the surface or the positive potential resulting from the overcharging of the EDL (**Fig. 4**).

Tetteh et al. (2024) investigated the EDL's structural characteristics at the silica–water interface, focusing on the orientation of water molecules and the hydrogen-bonding network. Using vSFG measurements, zeta potential analysis,

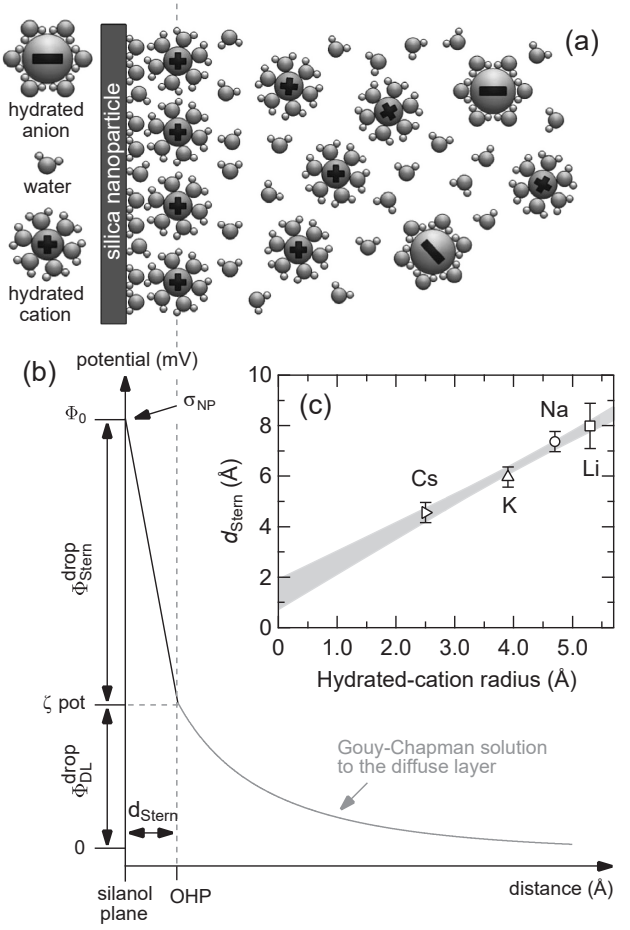

Fig. 3 Gouy–Chapman–Stern model of the electrical double layer. **(a)** The structure of the electrical double layer takes the form of a charged silanol plane and an outer Helmholtz plane (OHP), which represents the distance of closest approach of ions. A diffuse layer of hydrated ions sits outside the OHP, screening the net surface charge over a characteristic Debye length. **(b)** Surface potential is given by the potential drop across the Stern layer (bounded by the OHP) and the potential across the diffuse layer, the latter being given by the zeta potential. **(c)** Thickness of the Stern layer (d_{Stern}) as a function of hydrated cation radius, taking the reference potential Φ_0^{NaCl} to be –385 ± 20 mV. The linear fit has a *y* intercept at 1.4 ± 0.6 Å. Adapted with permission from Ref. (Brown et al., 2016). Copyright: (2016) American Physical Society.

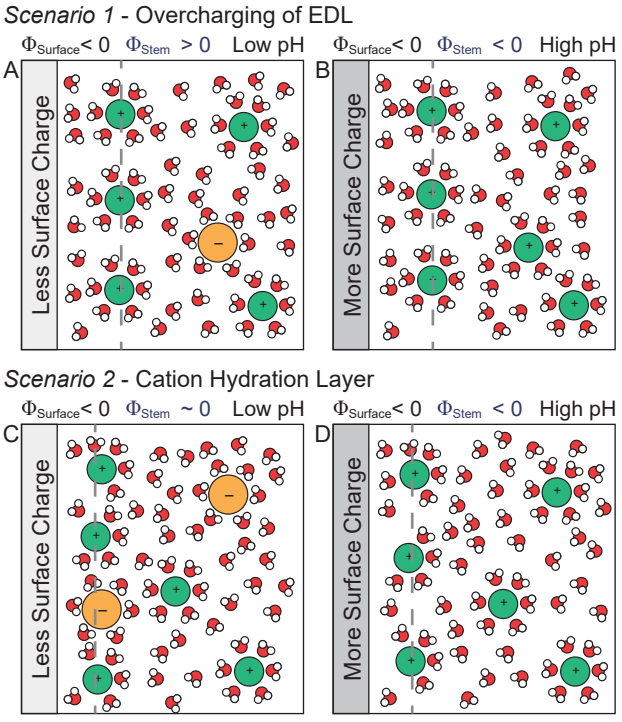

Fig. 4 Potential structures of the EDL that describe the behavior observed in the SFG intensity. Scenario 1 involves the overcharging of the EDL at low pH **(A)** and high pH **(B)**. Scenario 2 depicts the contribution of the cation hydration layer to the SFG at low pH **(C)** and high pH **(D)**. Adapted with permission from Ref. (Darlington et al., 2017). Copyright: (2017) American Chemical Society.

and the maximum entropy method, this study explored the effects of different cations (Li^+, Na^+, and Cs^+) at pH 2 (near-neutral surface) and pH 12 (highly charged surface) (**Fig. 5**). At pH 2, Li^+ and Na^+ disrupted existing water structure, while Cs^+ promoted greater order. At pH 12, the water orientation and ordering in the diffuse layer reversed, with Cs^+ enhancing ordering significantly. SIE trends varied between Stern and diffuse layers: Cs^+ facilitated stronger ordering in the Stern layer, while Na^+ and Li^+ had more pronounced effects in the diffuse layer. This divergence highlights the distinct SIE characteristics of the two layers. Water molecules' behavior in the Stern layer was pH-dependent, with changes in the order and orientation of the molecules as the pH shifted. Notably, Cs^+ promoted interlayer hydrogen bonding among water molecules, potentially contributing to the structural reversal at high pH values.

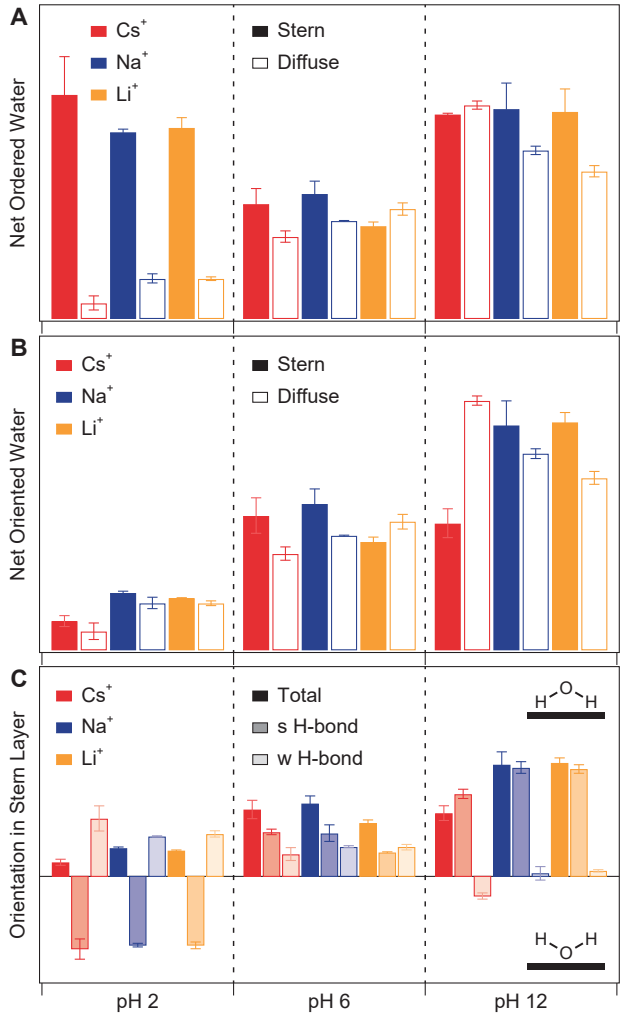

Fig. 5 Specific ion trends for the Stern and diffuse layers in **(A)** the average amount of net ordered water and **(B)** the average amount of net oriented water. **(C)** SIE trends in the net orientation of the Stern layer in terms of total water, the stronger hydrogen-bonded (s H-bond) and weakly hydrogen-bonded (w H-bond) networks. Adapted with permission from Ref. (Tetteh et al., 2024). Copyright: (2024) American Chemical Society.

Lovering et al. (2016) also reported that the structure of water molecules in the Stern layer at the silica–water interface depends on the identity of the cation. Using vSFG measurements, the authors investigated the effects of high-concentration salt solutions (NaCl, LiCl, $CaCl_2$, $MgCl_2$) and demonstrated that divalent cations (Mg^{2+}, Ca^{2+}) disrupt the ordered water structure more significantly than monovalent cations (Na^+, Li^+). They proposed a mechanism by which divalent cations generate a strong localized electrostatic field, inducing the hydrolysis of water molecules. The residual amount of ordered water observed correlated with the pK_a values of the cations ($Mg^{2+} < Ca^{2+} < Li^+ < Na^+$), revealing specific behaviors that cannot be fully explained by conventional EDL models.

3. SIEs on the electrokinetic phenomena of particles

Electrokinetic measurements (Delgado et al., 2007) have provided evidence of the ionic specificity of particle suspension systems. The preferential accumulation of chaotropic ions (structure-disrupting ions) and the exclusion of kosmotropic ions (structure-forming ions) on hydrophobic surfaces has been confirmed through electrophoretic mobility measurements conducted across various particle suspension systems (Calero et al., 2011; López-León et al., 2003, 2005, 2007, 2014; Scales et al., 1998).

3.1 The pH value of the dispersion medium, electrolyte concentration, and ion species

Saka and Güler (2006) investigated the effects of pH, electrolyte concentration, and ion species on the electrokinetic properties (zeta potential and electrokinetic charge density) of montmorillonite. The magnitude of the zeta potential of montmorillonite decreased as the concentration of monovalent electrolytes increased due to the compression of the EDL. Furthermore, the influence of the different monovalent ions followed the order $Li^+ > Na^+ > K^+ > Rb^+ > Cs^+$. In other words, ions with smaller hydration radii result in a greater reduction in the magnitude of the zeta potential. Furthermore, in the presence of multivalent ions ($CaCl_2$ and $AlCl_3$), the zeta potential transitioned from negative to neutral and eventually to positive as the concentration increased. For $AlCl_3$, the zeta potential reverted to a positive value when the concentration exceeded 0.5 mM. This change was attributed to the strong adsorption of Al^{3+} ions, which compressed the EDL.

3.2 Multiple anions

The effects of varying the concentration of multiple anions on the electrophoretic mobility and diffusion potential of magnetite nanoparticles were investigated through experiments and Monte Carlo simulations (Vereda et al., 2015). Electrophoretic mobility measurements were conducted at pH 4 with anion concentrations ranging from 5 to

200 mM. The results revealed that chaotropic anions (SCN^-, ClO_4^-) exhibited a limited effect in screening the positive surface charge of the particles, reducing mobility to values close to zero. In contrast, kosmotropic anions (SO_4^{2-}, $HC_6H_5O_7^{2-}$) effectively reversed the surface charge at low concentrations, causing a transition in mobility from positive to negative. This effect is particularly pronounced for citrate ions, which is attributed to their strong adsorption onto the iron oxide surface, resulting in the formation of metal-carboxylate surface complexes that facilitate charge reversal (Tombácz et al., 2013). The Monte Carlo simulations successfully replicated the experimentally observed SIEs, emphasizing the critical role of ionic polarizability and size in governing these behaviors.

3.3 Outer Helmholtz plane and slip length

Jalil and Pyell (2018) quantified the zeta potential and electrokinetic surface-charge density of amorphous silica nanoparticles depending on the type of counterions (Li^+, Na^+, K^+, and guanidinium ion (Gdm^+)) and their concentrations (20–120 mM). Specifically, they investigated the characteristics of the outer Helmholtz plane (OHP) and analyzed the influence of the hydration properties of the counterions on the EDL and surface-charge characteristics. OHP is traditionally denoted as the boundary between the Stern layer and the diffuse (outer) layer composed of mobile counterions, co-ions, and solvent molecules (Overbeek, 1965). The absolute value of the zeta potential decreased in the order of $Li^+ > Na^+ > K^+ > Gdm^+$, and demonstrated a decreasing trend with increasing counterion concentration. The comparison between the spherical and planar particle models provided insights into the influence of particle curvature on the electrokinetic properties. Moreover, the electrokinetic surface-charge density reflected the trends in the zeta potential, and the effects of the counterion type and concentration were manifested in the charge distribution across the OHP and Stern layers. Notably, Gdm^+, unlike other alkali metal ions, exhibits unique effects on the EDL owing to its weak hydration properties.

Fukasawa et al. (2020, 2021) investigated the effects of SIEs on the thickness of the slipping layer (slip length) using negatively charged hydrophobic polystyrene latex particles. The slip length is estimated to be several nanometers and plays a crucial role in electrokinetic behavior (Bhattacharyya and Majee, 2017; Gopmandal et al., 2017; Khair and Squires, 2009; Ohshima, 2004; Park, 2013; Zhao, 2010). Fukasawa et al. systematically examined the response of the ion distribution within the slipping layer and the electrophoretic mobility under various electrolyte concentrations (1, 10, and 50 mM) and electric field strengths. Under low electric field conditions, ions with smaller hydration radii such as Gdm^+ and Cs^+ accumulate more extensively within the slipping layer (**Fig. 6**). The ion accumulation within the slipping layer decreased as the electric field strength increased. In other words, ions with larger hydrated radii are less likely to accumulate within the slipping layer, leading to an increase in the magnitude of the electrophoretic mobility. Notably, Ph_4As^+, characterized by exceptionally strong hydrophobic interactions, formed a stable and highly concentrated layer within the slipping layer.

3.4 Hydrophilic and hydrophobic characteristics of particle surfaces

The impact of electrolytes containing alkali metal ions (Li^+, Na^+, K^+, Rb^+, Cs^+), chlorides, and sulfate anions on the electrosurface properties of hydrophobic (polystyrene latex with surface sulfate (PS-SO_3H) or carboxylic groups (PS-COOH)) and hydrophilic (SiO_2, ZrO_2, and bentonite) particles was investigated (Manilo et al., 2019). The

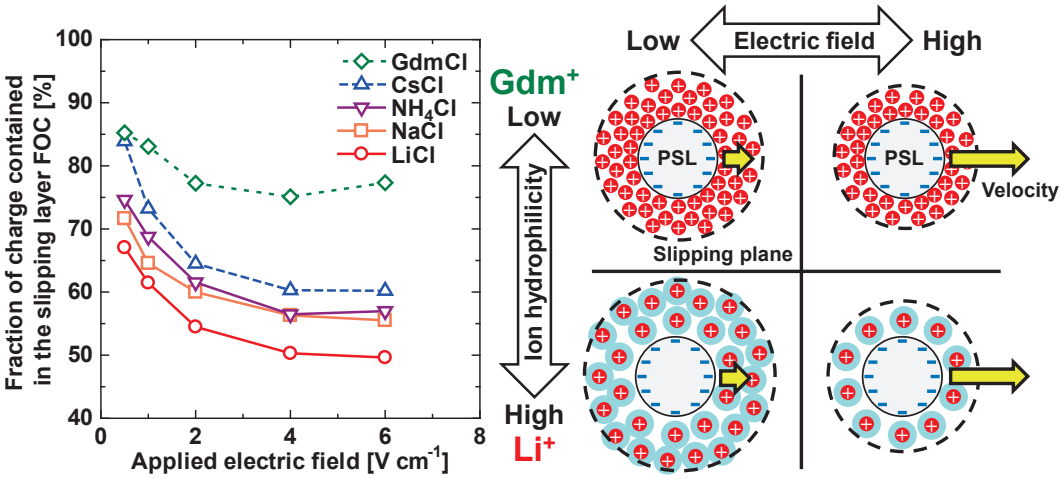

Fig. 6 Fraction of charge contained in the slipping layer of hydrophobic sulfate polystyrene latex particles with a diameter of 3.9 μm, as a function of the applied electric field in each electrolyte at a concentration of 50 mM. Adapted with permission from Ref. (Fukasawa et al., 2021). Copyright: (2021) Elsevier B.V.

behavior of the zeta potential was examined, revealing distinct maxima in the dependence: at electrolyte concentration = 0.1–1 mM for hydrophobic particles and 1–10 mM for hydrophilic particles. This phenomenon can be explained by two opposing effects: the polarization of the EDL, which increased the zeta potential at low electrolyte concentrations, and the compression of the EDL, which decreased the zeta potential at high concentrations. In concentrated solutions (> 1–10 mM), the magnitude of the zeta potential consistently decreased in accordance with direct HS along the sequence of Li^+ to Cs^+ cations. Conversely, in more dilute solutions, indirect HS was observed for certain particles (PS-COOH, SiO_2, and ZrO_2). This behavior likely reflects the phenomena related to the hydrophilic or hydrophobic nature of the surface, surface-charge density, and partial dehydration of the surface. The type of anion also affects the zeta potential. This behavior is attributed to the partial dehydration of the surface layer caused by sulfate ions, leading to a thinner hydration layer, a shift of the shear plane toward the surface, and an increase in the zeta potential. In addition, the relative electrical conductivities of both hydrophobic and hydrophilic suspensions demonstrated a consistent reduction in the contribution of EDL polarization (surface conductivity) along the HS (Dukhin, 1993; Garboczi and Douglas, 1996; Lyklema and Minor, 1998; Zhao, 2011). In general, the variations observed in the zeta potential and electrical conductivity across the HS were closely associated with the differences in the ionic properties, such as radius and mobility.

4. SIEs on the aggregation and dispersion properties of particle suspensions

The aggregation–dispersion characteristics and gelation behavior of particle suspensions were significantly influenced by SIEs. Studies on particle aggregation in electrolyte solutions have a long history, notably including the development of DLVO theory. This framework explains the behavior of charged colloidal particles at varying salt concentrations, predicting slow aggregation at low ionic strengths but rapid acceleration as the salt concentration increases. The critical transition is defined by the critical coagulation concentration (CCC), which is an important indicator of salt destabilizing power. A significant contribution of DLVO theory is its explanation of the Schulze–Hardy rule, which asserts that multivalent counterions significantly reduce CCC (Oncsik et al., 2014; Schneider et al., 2011). However, factors other than ion valence also influence CCC, one of the most well-studied being SIEs.

4.1 Aggregation characteristics and dispersion stabilization of particle suspensions

López-León et al. (2008) comprehensively investigated the stability of diverse colloidal systems using a low-angle light-scattering instrument. They employed polystyrene latex particles with various surface functional groups, including carboxyl, sulfonate, amine, and a combination of carboxyl and amine groups. In addition, protein-coated polystyrene particles were used to modify the surface hydrophobicity to partially hydrophilic, negatively charged hydrophilic silica particles, and positively charged hydrophilic chitosan particles. Furthermore, their research focused on representative cations (NH_4^+, Na^+, Ca^{2+}) and anions (SCN^-, NO_3^-, Cl^-) from the HS, which encompass a wide spectrum of properties ranging from chaotropic to kosmotropic behavior. Distinct HS were observed on hydrophobic surfaces with negative and positive charges. On negatively charged surfaces, weakly hydrated anions, such as SCN^-, were found to accumulate near the surface due to dispersion forces, thereby stabilizing the particles. Conversely, these anions destabilize positively charged surfaces. This reversal phenomenon can be explained by the dispersion force theory, which states that ion specificity is mainly determined by the polarity of ions in water (Boström et al., 2001, 2005, 2006; Kunz et al., 2004b; Ninham and Yaminsky, 1997; Salis et al., 2006). On hydrophilic surfaces, a partial HS reversal was observed, in contrast to the behavior observed on the hydrophobic surfaces. Hydrophilic surfaces strongly interact with surrounding water molecules, forming a densely structured water layer. This structured water layer promotes the exclusion of chaotropic anions, such as SCN^- and NO_3^-, while facilitating the accumulation of kosmotropic anions, such as Cl^-, near the surface. These results indicate that SCN^- and NO_3^- do not exhibit a stabilizing effect on hydrophilic surfaces; instead, they cause destabilization. López-León et al. discussed the phenomenon of restabilization. Restabilization is generally attributed to the presence of strongly hydrated cations, such as Ca^{2+}. These cations typically act as counterions that enhance the water structure near hydrophilic surfaces and form a steric barrier that prevents particle aggregation. The hydration forces responsible for restabilization become stronger with an increase in the hydration number of the cations (Jungwirth and Tobias, 2006; Molina-Bolívar et al., 1996, 1997, 1998; Molina-Bolívar and Ortega-Vinuesa, 1999). López-León et al. (2008) experimentally demonstrated that restabilization can be induced by cations and anions, including weakly hydrated ions such as SCN^- and NO_3^-. For a more detailed discussion, please refer to the original study.

The SIEs on the aggregation of negatively charged montmorillonite (K^+-montmorillonite) in various cation (Li^+, Na^+, K^+, Rb^+, Cs^+) solutions were quantitatively discussed using the activation energy as an indicator, based on an analysis of aggregation rates obtained through dynamic light-scattering measurements (Tian et al., 2014). The aggregation rate and CCC varied significantly depending on the cation type, with Li^+ exhibiting the highest CCC and Cs^+ showing the lowest CCC. The activation energy at

25 mM was highest for Li^+ and lowest for Cs^+. Furthermore, as the concentration decreased, the differences in the activation energies of the various cations became more pronounced. They also confirmed that the choice of anion (e.g., KNO_3 vs. KCl) only negligibly affected the aggregation dynamics and that cations played a dominant role in the aggregation process. In conclusion, the observed SIEs were primarily attributed to the polarization effect, where the strong electric field on the surface of the montmorillonite induced the deformation of the cation electron clouds.

The SIEs of monovalent ions on the surface charge and aggregation of anionic and cationic polystyrene latex particles were examined using electrophoresis and time-resolved light-scattering techniques (Oncsik et al., 2015). Weakly hydrated counterions, like $N(CH_3)_4^+$ and SCN^-, were strongly adsorbed onto oppositely charged surfaces, reducing the surface-charge magnitude and CCC. Strongly hydrated counterions such as Li^+ and F^- did not adsorb, resulting in high surface-charge magnitudes and elevated CCC values. The CCC values followed the HS for negatively charged sulfate latex particles, while exhibiting the reverse order for positively charged amidine latex particles. Co-ions with the same charge sign as the particle surface interact weakly with the surface, and the CCC is essentially independent of the nature of the co-ions. In the rapid aggregation regime, the aggregation rate was determined by the nature of the particles, with no significant influence from the specific type of ions.

Higashitani et al. (2017, 2018) measured the rapid aggregation rate of SiNPs using a low-angle light-scattering apparatus. Their study explored in detail the dependence of aggregation rates on the particle diameter and the type of co- and counterions in 1:1 electrolytes, with a particular focus on the Gibbs free energy of hydration. For particles with diameters of approximately 300 nm or less, the aggregation rate decreased exponentially as particle size decreased and as the magnitude of the Gibbs free energy of hydration for cations (counterions) and anions (co-ions) increased. The highly hydrated kosmotropic cation, Li^+, exhibits lower adsorption compared to the poorly hydrated chaotropic cation, Cs^+; however, it forms a thicker adsorbed layer, as schematically illustrated in **Fig. 7a**. The thicker adsorbed layer enhances the stability of colloidal particles by creating a structured cation layer that generates repulsive forces between colliding particles. Furthermore, the coagulation rate in potassium solutions is influenced by the Gibbs free energy of hydration of anions (co-ions). Potassium ions exhibit chaotropic properties. Highly chaotropic cations in concentrated solutions are likely excessively adsorbed onto the silica surface, leading to surface charge reversal (Dishon et al., 2009; Franks, 2002). Consequently, anions act as counterions on the silica surface coated with potassium ions. Similar to cations, anions act as structure-determining ions, and their degree of hydration is correlated with the thickness of the structured layer formed on the silica surface (**Fig. 7b**). Notably, silica nanoparticles with a diameter of 70 nm did not aggregate in 1 M KNO_3 and KSCN solutions. Nonspherical anions (NO_3^-, SCN^-), which exhibit weak cohesive interactions with potassium, formed fragile structures by randomly adsorbing onto the excess potassium layer present on the silica surface (**Fig. 7c**) (Li et al., 2005). Higashitani et al. proposed that these fragile structures are partially disrupted by strong van der Waals attractive forces in the case of larger particles, whereas in smaller particles where the van der Waals forces are too weak to destroy the structures, they act as strong repulsive forces.

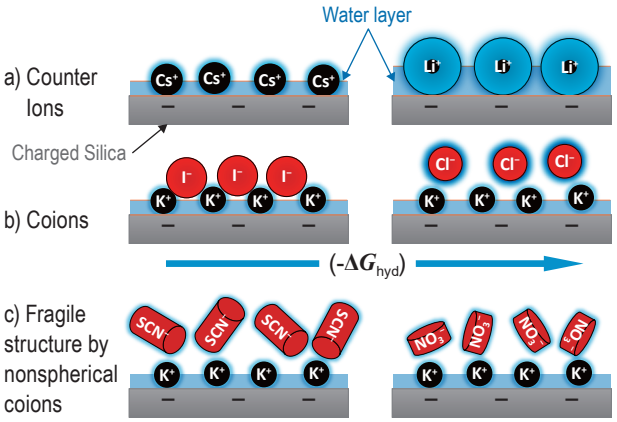

Fig. 7 Schematics of the adsorption of structure-determining ions. **(a)** Chaotropic Cs^+ ions adsorb excessively on the silica surface, and the kosmotropic Li^+ ions with the primary and secondary hydration shell form a thick adsorption layer to neutralize the silica surface. **(b)** Anions with different values of $(-\Delta G_{hyd})$ adsorb on the excessive potassium layer on the silica surface. **(c)** Nonspherical anions with weak cohesive energy to potassium make the fragile structure by adsorbing randomly on the excessive potassium layer on the silica surface. Adapted with permission from Ref. (Higashitani et al., 2018). Copyright: (2018) American Chemical Society.

4.2 Gelation of particle suspensions

The gelation of silica nanoparticles in mixtures of monovalent ions and in mixtures of divalent and monovalent ions was investigated (Sögaard et al., 2021). From the perspective of gelation time, monovalent-ion mixtures generally follow direct HS. For instance, compared with mixtures of Li and Na salts, mixtures of Li and K salts exhibited shorter gelation times, indicating that aggregation was promoted. In mixtures of divalent and monovalent ions, increasing the monovalent-ion concentration resulted in longer gelation times. This indicates that monovalent ions such as Li^+ and Na^+ can replace divalent ions like Mg^{2+} and Ca^{2+}, which exhibit strong interactions with the silica surface. Furthermore, the authors demonstrated that the HS of divalent ions at the silica interface is highly dependent on pH (**Fig. 8**). At pH below 9, the interaction between the silica surface and Mg^{2+} is weaker than that with

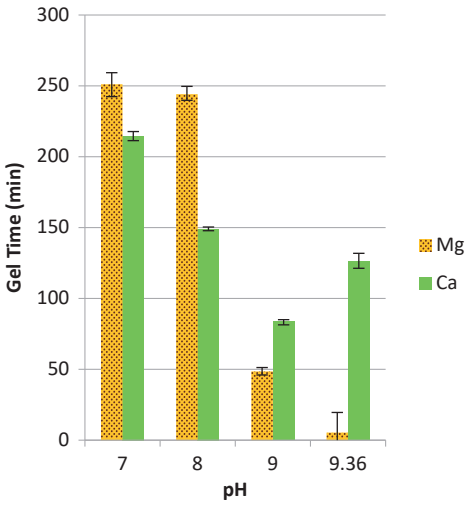

Fig. 8 Gel times of silica sols with $MgCl_2$ and $CaCl_2$ at various pH values. The original pH of the silica sol is 9.36. A shift in gel time can be observed for $MgCl_2$ at pH values less than 9, as it is longer than $CaCl_2$. Adapted with permission from Ref. (Sögaard et al., 2021). Copyright: (2021) Elsevier B.V.

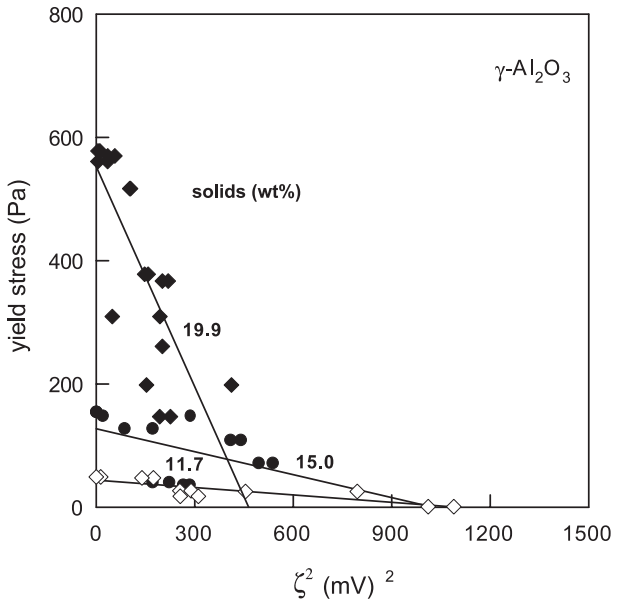

Fig. 9 Relationship between the yield stress and the squared zeta (ζ) potential for γ-Al_2O_3 dispersions. Adapted with permission from Ref. (Leong and Ong, 2003). Copyright: (2003) Elsevier B.V.

Ca^{2+}, following conventional HS. In contrast, an inversion of the HS was observed at pH values exceeding 9. This phenomenon is attributed to the charge and hydration characteristics of the silica surface: below pH 9, the weakly charged silica surface interacts more strongly with the relatively less hydrated Ca^{2+} than with Mg^{2+}. In contrast, above pH 9, the highly charged silica surface forms an ordered hydration layer, enhancing interactions with strongly hydrated ions such as Mg^{2+}. These findings are supported by molecular dynamics simulations (Sögaard et al., 2021; Sthoer et al., 2019).

5. SIEs on the rheological properties of particle suspensions

SIEs induce microscopic changes in ion accumulation structures, surface charges, electrokinetic behavior, and interparticle interactions. These microscopic changes, in turn, significantly affect the macroscopic properties, such as the rheology of particle suspensions (Johnson et al., 2000; Otsuki, 2018). This study primarily focused on shear yield stress, which is often referred to as static yield stress (Husband et al., 1993; Kelessidis and Maglione, 2008), as a rheological property of particle suspensions. The shear yield stress is the minimum applied stress required for viscoplastic materials to flow like a liquid, reflecting the internal structures of the suspension (Au et al., 2016) as well as the physical and chemical characteristics of the particles and dispersion medium. Several studies have been conducted on this topic. The vane method was used to measure the yield stress. It employs the vane geometry to measure the shear stress at a low shear rate over a certain period of time, identifying the maximum stress as the yield stress (Boger, 2009; Dzuy and Boger, 1983, 1985; Keentok, 1982).

5.1 Shear yield stress

The yield stress of homogeneously charged spherical particle suspensions was explained based on the DLVO theory, which describes interparticle interactions as the sum of van der Waals attractive forces and electrostatic double-layer repulsive forces. For instance, when the magnitude of the particle surface charge is small, the electrostatic double-layer repulsion has a reduced effect on the yield stress, whereas the van der Waals attractive forces become predominant, facilitating particle coagulation and consequently developing yield stress.

A research group at the University of Melbourne proposed a model that directly incorporates the DLVO theory into the yield stress by introducing a network structure term dependent on the particle size, solid volume fraction, and mean coordination number (Harbour et al., 2007a, 2007b; Johnson et al., 2000; Kapur et al., 1997; Scales et al., 1998). Fundamentally, based on the DLVO theory, at the isoelectric point (IEP), where the zeta potential appears to be zero, the electrostatic repulsive forces disappear, resulting in the maximum yield stress. Notably, if particle–particle interactions are exclusively governed by DLVO interactions, then a linear correlation is expected between the yield stress and the square of the zeta potential (Firth, 1976). Leong and Ong (2003) suggested that the intercept of an extrapolated line with the square axis of the zeta potential represents the square of the critical zeta potential (**Fig. 9**). The critical zeta potential marks the transition between aggregation and dispersion. Specifically, particles

tend to aggregate when the zeta potential is below this critical value, whereas they remain dispersed above it owing to electrostatic repulsive forces. However, various studies have demonstrated that the linear relationship between the yield stress and the square of the zeta potential based on the DLVO theory is not universally applicable to all systems. Gustafsson et al. (2000) investigated the effects of pH (3–10) and NaCl concentration (0–1 M) on the yield stress and zeta potential of anatase (TiO_2) dispersions. Their findings revealed that in the acidic branch below the isoelectric point, a linear relationship consistent with the theoretical predictions was observed, whereas in the alkaline branch, particularly at high electrolyte concentrations, no such linear relationship was observed. Teh et al. (2009) examined the influence of surface chemistry on yield stress using slurries prepared from two types of kaolin clay. Their study highlighted that even with similar mineral compositions, clay minerals often exhibit variations in the surface chemistry of particle edges, leading to distinct rheological and electrokinetic behaviors (Adachi et al., 2020; Johnson et al., 2000; Otsuki, 2018; Stul and Mortier, 1974). They employed small anionic additives such as citric acid to homogenize the surface chemistry of the particle edges, achieving similar yield stress–pH behaviors across different kaolin clay slurries.

The deviation from the linear relationship between the yield stress and the square of the zeta potential arises from the presence of non-DLVO interaction forces (Israelachvili, 2011). For example, under high electrolyte concentrations, ion–ion interactions, which are neglected in classical DLVO theory, become significant.

Johnson et al. (1999) reported that the yield stress of α-alumina particle (median diameter of 300 nm) in 1 M nitrate electrolyte increased depending on the type of monovalent cation in the following order $Cs^+ < K^+ < Na^+ < Li^+$ (**Fig. 10**). They focused on the impact of ion species on the interparticle distance, as the contribution of van der Waals forces becomes relatively more significant when the interparticle distance decreases. Thus, highly hydrated cations (e.g., Li^+) could approach the α-alumina surface more closely, thereby reducing the interparticle distance, which enhanced the contribution of attractive forces and resulted in increased yield stress.

Franks (2002) reported the effect of monovalent cation species on the yield stress of submicron-sized silica particle suspensions in chloride electrolytes. He demonstrated that the maximum yield stress increased in the following order $Li^+ < Na^+ < K^+ < Cs^+$, which was the reverse of that observed for α-alumina (**Fig. 11**). Furthermore, the pH at the maximum yield stress did not correspond to the IEP of the silica particles (pH = 2) and shifted to higher pH values in the following order: $Li^+ < Na^+ < K^+ < Cs^+$, similar to the maximum yield stress. The observed results were explained based on two factors. The first is the reduction in EDL repulsion caused by the neutralization of particle surface charges in solutions containing the least hydrated cations (e.g., Cs^+). The second is the additional attraction arising from ion adsorption (ion–ion correlation forces) (Guldbrand et al., 1984; Israelachvili, 2011; Kjellander, 1996).

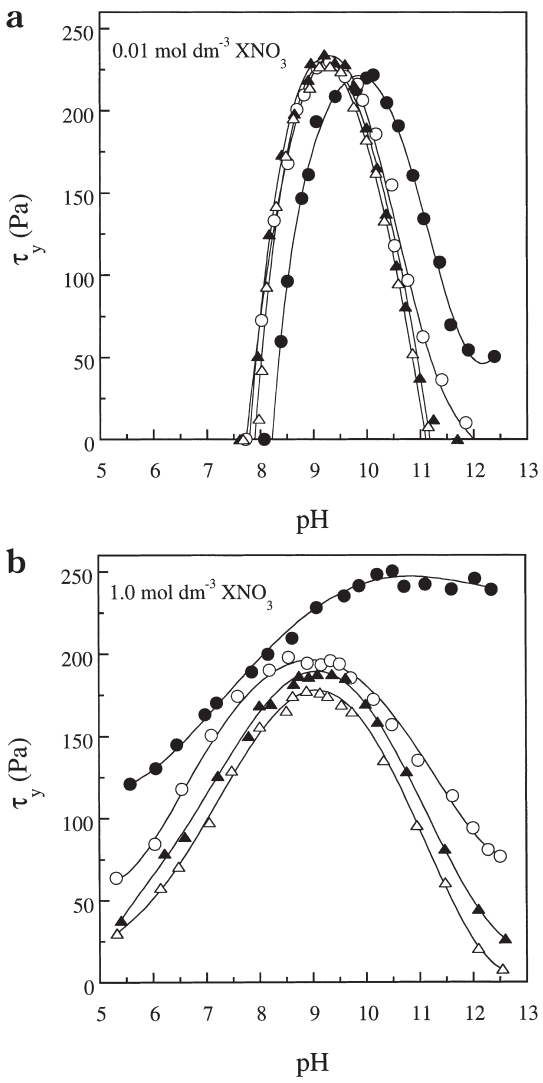

Fig. 10 Shear yield stress (τ_y) behavior of α-alumina suspensions as a function of monovalent cation type and pH. The electrolyte concentration is **(a)** 0.01 mol dm^{-3} XNO_3 and **(b)** 1.0 mol dm^{-3} XNO_3. The alumina volume fraction is 0.250 in all cases. Key: (●) X = Li; (○) X = Na; (▲) X = K; (△) X = Cs. Adapted with permission from Ref. (Johnson et al., 1999). Copyright: (1999) American Chemical Society.

Parsons et al. (2010) discussed the completely contrasting trend observed between α-alumina and silica suspensions in chloride electrolytes based on a modified Poisson–Boltzmann analysis. This analysis incorporates hydration effects into non-electrostatic ion–surface dispersion interactions based on ionic excess polarization and finite ion sizes. The EDL pressure between the particles revealed a direct HS ($K^+ > Na^+ > Li^+$) for silica surfaces and a reversed series ($Li^+ > Na^+ > K^+$) for alumina surfaces, which aligned the theoretical predictions with the experimental observations (with higher pressure

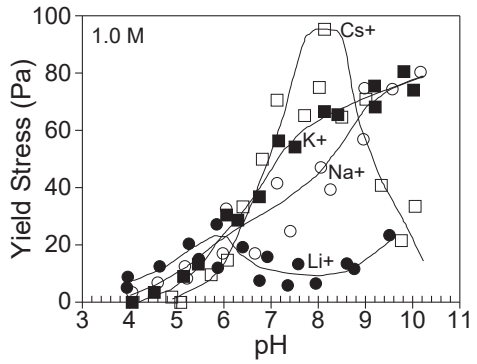

Fig. 11 Yield stresses of 40 vol% Geltech silica in 1.0 M chloride solution. The counterions are as indicated in the figure. Adapted with permission from Ref. (Franks, 2002). Copyright: (2002) Elsevier B.V.

corresponding to lower yield stress). Furthermore, calculations using unhydrated ions suggest the possibility of surface-induced dehydration on alumina surfaces.

5.2 Interaction and frictional forces

AFM measurements of the adsorption and short-range interactions between silica colloid and mica surface in monovalent chloride electrolyte solutions revealed a significant SIE (Vakarelski et al., 2000; Vakarelski and Higashitani, 2001). Highly hydrated ions (Li^+, Na^+) exhibit strong adhesive forces, whereas weak adhesion is observed for poorly hydrated ions (K^+, Cs^+). Donose et al. (2005) investigated the effects of various monovalent cations on the friction between silica surfaces using AFM. Their results revealed that smaller, strongly hydrated cations (Li^+) exhibited superior lubrication performance compared to layers of larger, weakly hydrated cations (Cs^+) (**Fig. 12**). Interestingly, unlike the case of a silica colloid interacting with a mica surface (Vakarelski et al., 2000; Vakarelski and Higashitani, 2001), no adhesion was observed. This result suggests that the interaction mechanisms at very short separations differ between silica-on-mica and silica-on-silica systems. Dishon et al. (2009) investigated the interactions between silica surfaces in monovalent chloride electrolyte solutions using AFM. Their findings demonstrated that specific cation adsorption directly affects the neutralization and reversal of the surface charge, the suppression of electrostatic double-layer repulsion, and the emergence of van der Waals attraction. The adsorption increased monotonically in the order $Cs^+ > K^+ > Na^+$, following the bare ionic radii of the cations. This trend reflects the influence of the hydration shells on the charged silica surface, suggesting that larger cations lose their hydration shells more readily and are adsorbed onto the surface. Their results were consistent with the HS observed in the rheological experiments.

This study focused on the shear yield stress as a key rheological property of particle suspensions and provided an overview of previous studies. For further insights into

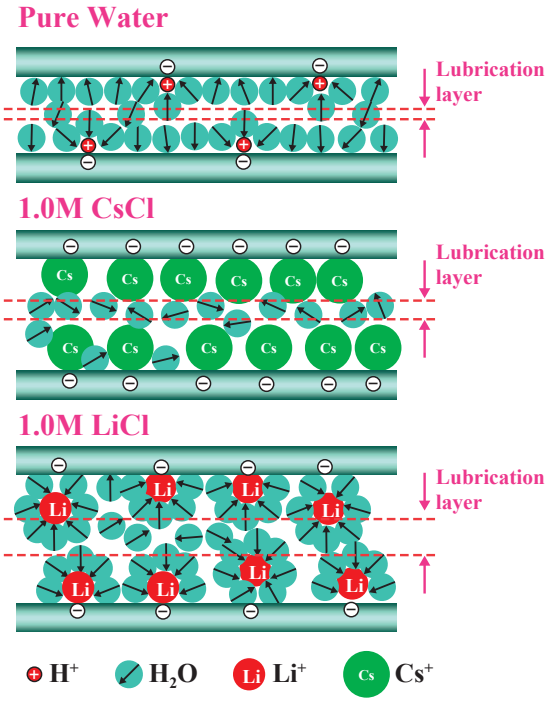

Fig. 12 Schematic representation of hypothetical frictional mechanisms. Adapted with permission from Ref. (Donose et al., 2005). Copyright: (2005) American Chemical Society.

the effects of SIEs on the shear viscosity, compressive yield stress, and viscoelastic behavior, readers are encouraged to refer to the cited references (Channell and Zukoski, 1997; Colic et al., 1998; Jeldres et al., 2019; Johnson et al., 2000; Quezada et al., 2017; Zhou et al., 2001).

6. Conclusions

This review provides an overview of SIEs in particle suspension systems, emphasizing their fundamental and applied significance. By exploring phenomena such as electrokinetic behavior, aggregation–dispersion characteristics, and rheological properties, the interplay between ion identity and particle surface interactions is highlighted. These findings underscore the importance of accounting for SIEs across various disciplines, including chemical, industrial, agricultural, environmental, biological, and medical sciences. SIEs are highly sensitive to slight variations in experimental conditions, which fosters academic interest and complicates the establishment of a theoretical framework, thus emphasizing the need for multifaceted evaluation. Although not extensively discussed in this review, the impact of SIEs on the structural formation, mechanical strength, deformation of particle aggregates, and suspension internal structures, as well as their influence on gelation behavior and viscoelastic properties, are crucial topics. Furthermore, the effects of nonaqueous systems and organic ions on SIEs remain important areas of study, with potential for further advancement.

Acknowledgments

This work was supported by JSPS KAKENHI, Grant Numbers JP23K04397 and JP20K05194, the Hosokawa Powder Technology Foundation (HPTF23301), and the Information Center of Particle Technology, Japan.

Nomenclature

AFM	Atomic force microscope
CCC	Critical coagulation concentration
DH	Debye–Hückel
EDL	Electrical double layer
HS	Hofmeister series
IEP	Isoelectric point
OHP	Outer Helmholtz plane
PMF	Potential of mean force
PZC	Point of zero charge
SIE	Specific ion effect
vSFG	vibrational sum-frequency generation
d_{Stern}	thickness of the Stern layer
ΔG_{hyd}	Gibbs free hydration energy
Φ_0	reference potential

References

Adachi Y., Kawashima Y.T., Ghazali M.E. Bin, Rheology and sedimentation of aqueous suspension of Na-montmorillonite in the very dilute domain, KONA Powder and Particle Journal, 37 (2020) 145–165. https://doi.org/10.14356/KONA.2020019

Au P.-I., Liu J., Leong Y.-K., Yield stress and microstructure of washed oxide suspensions at the isoelectric point: experimental and model fractal structure, Rheologica Acta, 55 (2016) 847–856. https://doi.org/10.1007/s00397-016-0959-y

Bastos-González D., Pérez-Fuentes L., Drummond C., Faraudo J., Ions at interfaces: the central role of hydration and hydrophobicity, Current Opinion in Colloid & Interface Science, 23 (2016) 19–28. https://doi.org/10.1016/J.COCIS.2016.05.010

Bhattacharyya S., Majee P.S., Electrophoresis of a polarizable charged colloid with hydrophobic surface: a numerical study, Physical Review E, 95 (2017) 042605. https://doi.org/10.1103/PhysRevE.95.042605

Boger D.V., Rheology and the resource industries, Chemical Engineering Science, 64 (2009) 4525–4536. https://doi.org/10.1016/j.ces.2009.03.007

Boström M., Deniz V., Franks G.V., Ninham B.W., Extended DLVO theory: electrostatic and non-electrostatic forces in oxide suspensions, Advances in Colloid and Interface Science, 123–126 (2006) 5–15. https://doi.org/10.1016/J.CIS.2006.05.001

Boström M., Tavares F.W., Finet S., Skouri-Panet F., Tardieu A., Ninham B.W., Why forces between proteins follow different Hofmeister series for pH above and below pI, Biophysical Chemistry, 117 (2005) 217–224. https://doi.org/10.1016/J.BPC.2005.05.010

Boström M., Williams D.R.M., Ninham B.W., Specific ion effects: why dlvo theory fails for biology and colloid systems, Physical Review Letters, 87 (2001) 168103/1-168103/4. https://doi.org/10.1103/PhysRevLett.87.168103

Brown M.A., Abbas Z., Kleibert A., Green R.G., Goel A., May S., Squires T.M., Determination of surface potential and electrical double-layer structure at the aqueous electrolyte-nanoparticle interface, Physical Review X, 6 (2016) 011007. https://doi.org/10.1103/PhysRevX.6.011007

Bunton C.A., Nome F., Quina F.H., Romsted L.S., Ion binding and reactivity at charged aqueous interfaces, Accounts of Chemical Research, 24 (1991) 357–364. https://doi.org/10.1021/ar00012a001

Calero C., Faraudo J., Bastos-González D., Interaction of monovalent ions with hydrophobic and hydrophilic colloids: charge inversion and ionic specificity, Journal of the American Chemical Society, 133 (2011) 15025–15035. https://doi.org/10.1021/ja204305b

Channell G.M., Zukoski C.F., Shear and compressive rheology of aggregated alumina suspensions, AIChE Journal, 43 (1997) 1700–1708. https://doi.org/10.1002/AIC.690430707

Colic M., Fisher M.L., Franks G.V., Influence of ion size on short-range repulsive forces between silica surfaces, Langmuir, 14 (1998) 6107–6112. https://doi.org/10.1021/la980489y

Collins K.D., Charge density-dependent strength of hydration and biological structure, Biophysical Journal, 72 (1997) 65–76. https://doi.org/10.1016/S0006-3495(97)78647-8

Collins K.D., Neilson G.W., Enderby J.E., Ions in water: characterizing the forces that control chemical processes and biological structure, Biophysical Chemistry, 128 (2007) 95–104. https://doi.org/10.1016/J.BPC.2007.03.009

Collins K.D., Washabaugh M.W., The Hofmeister effect and the behaviour of water at interfaces, Quarterly Reviews of Biophysics, 18 (1985) 323–422. https://doi.org/10.1017/S0033583500005369

Darlington A.M., Jarisz T.A., Dewalt-Kerian E.L., Roy S., Kim S., Azam M.S., Hore D.K., Gibbs J.M., Separating the pH-dependent behavior of water in the stern and diffuse layers with varying salt concentration, The Journal of Physical Chemistry C, 121 (2017) 20229–20241. https://doi.org/10.1021/acs.jpcc.7b03522

Delgado A.V., González-Caballero F., Hunter R.J., Koopal L.K., Lyklema J., Measurement and interpretation of electrokinetic phenomena, Journal of Colloid and Interface Science, 309 (2007) 194–224. https://doi.org/10.1016/J.JCIS.2006.12.075

Dishon M., Zohar O., Sivan U., From repulsion to attraction and back to repulsion: the effect of NaCl, KCl, and CsCl on the force between silica surfaces in aqueous solution, Langmuir, 25 (2009) 2831–2836. https://doi.org/10.1021/la803022b

Donose B.C., Vakarelski I.U., Higashitani K., Silica surfaces lubrication by hydrated cations adsorption from electrolyte solutions, Langmuir, 21 (2005) 1834–1839. https://doi.org/10.1021/la047609o

dos Santos A.P., Diehl A., Levin Y., Surface tensions, surface potentials, and the Hofmeister series of electrolyte solutions, Langmuir, 26 (2010) 10778–10783. https://doi.org/10.1021/la100604k

Dukhin S.S., Non-equilibrium electric surface phenomena, Advances in Colloid and Interface Science, 44 (1993) 1–134. https://doi.org/10.1016/0001-8686(93)80021-3

Dumont F., Warlus J., Watillon A., Influence of the point of zero charge of titanium dioxide hydrosols on the ionic adsorption sequences, Journal of Colloid and Interface Science, 138 (1990) 543–554. https://doi.org/10.1016/0021-9797(90)90236-H

Dzuy N.Q., Boger D.V., Yield stress measurement for concentrated suspensions, Journal of Rheology, 27 (1983) 321–349. https://doi.org/10.1122/1.549709

Dzuy N.Q., Boger D.V., Direct yield stress measurement with the vane method, Journal of Rheology, 29 (1985) 335–347. https://doi.org/10.1122/1.549794

Firth B.A., Flow properties of coagulated colloidal suspensions: ii. experimental properties of the flow curve parameters, Journal of Colloid and Interface Science, 57 (1976) 257–265. https://doi.org/10.1016/0021-9797(76)90201-0

Franks G.V., Zeta potentials and yield stresses of silica suspensions in concentrated monovalent electrolytes: isoelectric point shift and additional attraction, Journal of Colloid and Interface Science, 249 (2002) 44–51. https://doi.org/10.1006/JCIS.2002.8250

Freire M.G., Carvalho P.J., Silva A.M.S., Santos L.M.N.B.F., Rebelo L.P.N., Marrucho I.M., Coutinho J.A.P., Ion specific effects on the mutual solubilities of water and hydrophobic ionic liquids, The Journal of Physical Chemistry B, 113 (2009) 202–211. https://doi.org/10.1021/jp8080035

Fukasawa T., Maruyama N., Ono K., Ishigami T., Fukui K., Effect of ion species on change in particle electrophoresis caused by change in applied electric field, Colloid and Interface Science Communications, 43 (2021) 100462. https://doi.org/10.1016/J.COLCOM.2021.100462

Fukasawa T., Ono K., Ishigami T., Fukui K., Electrophoretic classification based on differences in electrophoretic mobility caused by change in the applied electric field, Powder Technology, 362 (2020) 586–590. https://doi.org/10.1016/j.powtec.2019.12.027

Garboczi E.J., Douglas J.F., Intrinsic conductivity of objects having arbitrary shape and conductivity, Physical Review E, 53 (1996) 6169–6180. https://doi.org/10.1103/PhysRevE.53.6169

Gopmandal P.P., Bhattacharyya S., Ohshima H., On the similarity between the electrophoresis of a liquid drop and a spherical hydrophobic particle, Colloid and Polymer Science, 295 (2017) 2077–2082. https://doi.org/10.1007/s00396-017-4181-y

Gregory K.P., Elliott G.R., Robertson H., Kumar A., Wanless E.J., Webber G.B., Craig V.S.J., Andersson G.G., Page A.J., Understanding specific ion effects and the Hofmeister series, Physical Chemistry Chemical Physics, 24 (2022) 12682–12718. https://doi.org/10.1039/D2CP00847E

Gregory K.P., Wanless E.J., Webber G.B., Craig V.S.J., Page A.J., The electrostatic origins of specific ion effects: quantifying the Hofmeister series for anions, Chemical Science, 12 (2021) 15007–15015. https://doi.org/10.1039/D1SC03568A

Gregory K.P., Webber G.B., Wanless E.J., Page A.J., Lewis strength determines specific-ion effects in aqueous and nonaqueous solvents, The Journal of Physical Chemistry A, 123 (2019) 6420–6429. https://doi.org/10.1021/acs.jpca.9b04004

Guldbrand L., Jönsson B., Wennerström H., Linse P., Phys Lett A., JOnsson B., WennerstrOm Ha., Electrical double layer forces. A Monte Carlo study, The Journal of Chemical Physics, 80 (1984) 2221–2228. https://doi.org/10.1063/1.446912

Gustafsson J., Mikkola P., Jokinen M., Rosenholm J.B., The influence of pH and NaCl on the zeta potential and rheology of anatase dispersions, Colloids and Surfaces A: Physicochemical and Engineering Aspects, 175 (2000) 349–359. https://doi.org/10.1016/S0927-7757(00)00634-8

Harbour P.J., Dixon D.R., Scales P.J., The role of natural organic matter in suspension stability 2. Modelling of particle–particle interaction, Colloids and Surfaces A: Physicochemical and Engineering Aspects, 295 (2007a) 67–74. https://doi.org/10.1016/j.colsurfa.2006.08.032

Harbour P.J., Dixon D.R., Scales P.J., The role of natural organic matter in suspension stability 1. Electrokinetic–rheology relationships, Colloids and Surfaces A: Physicochemical and Engineering Aspects, 295 (2007b) 38–48. https://doi.org/10.1016/j.colsurfa.2006.08.028

Higashitani K., Nakamura K., Fukasawa T., Tsuchiya K., Mori Y., Ionic specificity in rapid coagulation of silica nanoparticles, Langmuir, 34 (2018) 2505–2510. https://doi.org/10.1021/acs.langmuir.7b04081

Higashitani K., Nakamura K., Shimamura T., Fukasawa T., Tsuchiya K., Mori Y., Orders of magnitude reduction of rapid coagulation rate with decreasing size of silica nanoparticles, Langmuir, 33 (2017) 5046–5051. https://doi.org/10.1021/acs.langmuir.7b00932

Hofmeister F., Zur Lehre von der Wirkung der Salze - Dritte Mittheilung, Archiv für Experimentelle Pathologie und Pharmakologie, 25 (1888) 1–30. https://doi.org/10.1007/BF01838161

Huang D.M., Cottin-Bizonne C., Ybert C., Bocquet L., Aqueous electrolytes near hydrophobic surfaces: dynamic effects of ion specificity and hydrodynamic slip, Langmuir, 24 (2008) 1442–1450. https://doi.org/10.1021/la7021787

Husband D.M., Aksel N., Gleissle W., The existence of static yield stresses in suspensions containing noncolloidal particles, Journal of Rheology, 37 (1993) 215–235. https://doi.org/10.1122/1.550442

Israelachvili J.N., Intermolecular and Surface Forces, 3rd Edition, Academic Press, 2011, ISBN: 978-0-12-375182-9. https://doi.org/10.1016/C2009-0-21560-1

Jalil A.H., Pyell U., Quantification of Zeta-potential and electrokinetic surface charge density for colloidal silica nanoparticles dependent on type and concentration of the counterion: probing the outer Helmholtz plane, The Journal of Physical Chemistry C, 122 (2018) 4437–4453. https://doi.org/10.1021/acs.jpcc.7b12525

Jeldres R.I., Piceros E.C., Leiva W.H., Toledo P.G., Quezada G.R., Robles P.A., Valenzuela J., Analysis of silica pulp viscoelasticity in saline media: the effect of cation size, Minerals, 9 (2019) 1–15. https://doi.org/10.3390/min9040216

Jiang Y., Tang R., Duncan B., Jiang Z., Yan B., Mout R., Rotello V.M., Direct cytosolic delivery of siRNA using nanoparticle-stabilized nanocapsules, Angewandte Chemie International Edition, 54 (2015) 506–510. https://doi.org/10.1002/anie.201409161

Johnson S.B., Franks G.V., Scales P.J., Boger D.V., Healy T.W., Surface chemistry–rheology relationships in concentrated mineral suspensions, International Journal of Mineral Processing, 58 (2000) 267–304. https://doi.org/10.1016/S0301-7516(99)00041-1

Johnson S.B., Franks G.V., Scales P.J., Healy T.W., The binding of monovalent electrolyte ions on α-alumina. ii. the shear yield stress of concentrated suspensions, Langmuir, 15 (1999) 2844–2853. https://doi.org/10.1021/la9808768

Jungwirth P., Tobias D.J., Specific ion effects at the air/water interface, Chemical Reviews, 106 (2006) 1259–1281. https://doi.org/10.1021/cr0403741

Kapur P.C., Scales P.J., Boger D.V., Healy T.W., Yield stress of suspensions loaded with size distributed particles, AIChE Journal, 43 (1997) 1171–1179. https://doi.org/10.1002/AIC.690430506

Keentok M., The measurement of the yield stress of liquids, Rheologica Acta, 21 (1982) 325–332. https://doi.org/10.1007/BF01515720

Kelessidis V.C., Maglione R., Yield stress of water-bentonite dispersions, Colloids and Surfaces A: Physicochemical and Engineering Aspects, 318 (2008) 217–226. https://doi.org/10.1016/j.colsurfa.2007.12.050

Khair A.S., Squires T.M., The influence of hydrodynamic slip on the electrophoretic mobility of a spherical colloidal particle, Physics of Fluids, 21 (2009) 042001. https://doi.org/10.1063/1.3116664

Kjellander R., Ion-ion correlations effective charges in electrolyte and macroion systems, Berichte der Bunsengesellschaft für physikalische Chemie, 100 (1996) 894–904. https://doi.org/10.1002/BBPC.19961000635

Kunz W., Henle J., Ninham B.W., 'Zur Lehre von der Wirkung der Salze' (about the science of the effect of salts): Franz Hofmeister's historical papers, Current Opinion in Colloid & Interface Science, 9 (2004a) 19–37. https://doi.org/10.1016/J.COCIS.2004.05.005

Kunz W., Lo Nostro P., Ninham B.W., The present state of affairs with Hofmeister effects, Current Opinion in Colloid & Interface Science, 9 (2004b) 1–18. https://doi.org/10.1016/J.COCIS.2004.05.004

Labban A.K.S., Marcus Y., The solubility and solvation of salts in mixed nonaqueous solvents. 1. potassium halides in mixed aprotic solvents, Journal of Solution Chemistry, 20 (1991) 221–232. https://doi.org/10.1007/BF00649530

Labban A.K.S., Marcus Y., The solubility and solvation of salts in mixed nonaqueous solvents. 2. potassium halides in mixed protic solvents, Journal of Solution Chemistry, 26 (1997) 1–12. https://doi.org/10.1007/BF02439440

Leong Y.K., Ong B.C., Critical zeta potential and the Hamaker constant of oxides in water, Powder Technology, 134 (2003) 249–254. https://doi.org/10.1016/j.powtec.2003.08.054

Leontidis E., Investigations of the Hofmeister series and other specific ion effects using lipid model systems, Advances in Colloid and Interface Science, 243 (2017) 8–22. https://doi.org/10.1016/J.CIS.2017.04.001

Levin Y., Santos A.P. dos, Ions at hydrophobic interfaces, Journal of Physics: Condensed Matter, 26 (2014) 203101. https://doi.org/10.1088/0953-8984/26/20/203101

Li Y., Kanda Y., Shinto H., Vakarelski I.U., Higashitani K., Fragile structured layers on surfaces in highly concentrated solutions of electrolytes of various valencies, Colloids and Surfaces A: Physicochemical and Engineering Aspects, 260 (2005) 39–43. https://doi.org/10.1016/j.colsurfa.2005.02.016

López-León T., Elaïssari A., Ortega-Vinuesa J.L., Bastos-González D., Hofmeister effects on poly(NIPAM) microgel particles: macroscopic evidence of ion adsorption and changes in water structure, ChemPhysChem, 8 (2007) 148–156. https://doi.org/10.1002/cphc.200600521

López-León T., Jódar-Reyes A.B., Bastos-González D., Ortega-Vinuesa J.L., Hofmeister effects in the stability and electrophoretic mobility of polystyrene latex particles, The Journal of Physical Chemistry B, 107 (2003) 5696–5708. https://doi.org/10.1021/jp0216981

López-León T., Jódar-Reyes A.B., Ortega-Vinuesa J.L., Bastos-González D., Hofmeister effects on the colloidal stability of an IgG-coated polystyrene latex, Journal of Colloid and Interface Science, 284 (2005) 139–148. https://doi.org/10.1016/j.jcis.2004.10.021

López-León T., Ortega-Vinuesa J.L., Bastos-González D., Elaissari A., Thermally sensitive reversible microgels formed by poly(N-

Isopropylacrylamide) charged chains: a Hofmeister effect study, Journal of Colloid and Interface Science, 426 (2014) 300–307. https://doi.org/10.1016/J.JCIS.2014.04.020

López-León T., Santander-Ortega M.J., Ortega-Vinuesa J.L., Bastos-González D., Hofmeister effects in colloidal systems: Influence of the surface nature, The Journal of Physical Chemistry C, 112 (2008) 16060–16069. https://doi.org/10.1021/JP803796A

Lovering K.A., Bertram A.K., Chou K.C., New information on the ion-identity-dependent structure of stern layer revealed by sum frequency generation vibrational spectroscopy, The Journal of Physical Chemistry C, 120 (2016) 18099–18104. https://doi.org/10.1021/acs.jpcc.6b05564

Lyklema J., Fundamentals of Interface and Colloid Science, Volume II, Solid-Liquid Interfaces, Academic Press, 1995, ISBN: 9780124605244.

Lyklema J., Lyotropic sequences in colloid stability revisited, Advances in Colloid and Interface Science, 100–102 (2003) 1–12. https://doi.org/10.1016/S0001-8686(02)00075-1

Lyklema J., Simple Hofmeister series, Chemical Physics Letters, 467 (2009) 217–222. https://doi.org/10.1016/j.cplett.2008.11.013

Lyklema J., Minor M., On surface conduction and its role in electrokinetics, Colloids and Surfaces A: Physicochemical and Engineering Aspects, 140 (1998) 33–41. https://doi.org/10.1016/S0927-7757(97)00266-5

Manilo M.V., Lebovka N.I., Barany S., Effects of sort and concentration of salts on the electrosurface properties of aqueous suspensions containing hydrophobic and hydrophilic particles: validity of the Hofmeister series, Journal of Molecular Liquids, 276 (2019) 875–884. https://doi.org/10.1016/j.molliq.2018.12.058

Mazzini V., Craig V.S.J., Specific-ion effects in non-aqueous systems, Current Opinion in Colloid & Interface Science, 23 (2016) 82–93. https://doi.org/10.1016/J.COCIS.2016.06.009

Molina-Bolívar J.A., Galisteo-González F., Hidalgo-Alvarez R., Stabilization of protein-latex complexes at high ionic strength, Colloids and Surfaces B: Biointerfaces, 8 (1996) 73–80. https://doi.org/10.1016/S0927-7765(96)01310-0

Molina-Bolívar J.A., Galisteo-González F., Hidalgo-Álvarez R., Colloidal stability of protein-polymer systems: a possible explanation by hydration forces, Physical Review E, 55 (1997) 4522–4530. https://doi.org/10.1103/PhysRevE.55.4522

Molina-Bolívar J.A., Galisteo-González F., Hidalgo-Álvarez R., Anomalous colloidal stability of latex-protein systems, Journal of Colloid and Interface Science, 206 (1998) 518–526. https://doi.org/10.1006/JCIS.1998.5679

Molina-Bolívar J.A., Ortega-Vinuesa J.L., How proteins stabilize colloidal particles by means of hydration forces, Langmuir, 15 (1999) 2644–2653. https://doi.org/10.1021/la981445s

Morag J., Dishon M., Sivan U., The governing role of surface hydration in ion specific adsorption to silica: an AFM-based account of the Hofmeister universality and its reversal, Langmuir, 29 (2013) 6317–6322. https://doi.org/10.1021/la400507n

Nihonyanagi S., Yamaguchi S., Tahara T., Water hydrogen bond structure near highly charged interfaces is not like ice, Journal of the American Chemical Society, 132 (2010) 6867–6869. https://doi.org/10.1021/ja910914g

Ninham B.W., Yaminsky V., Ion binding and ion specificity: the Hofmeister effect and Onsager and Lifshitz theories, Langmuir, 13 (1997) 2097–2108. https://doi.org/10.1021/la960974y

Ohshima H., Electrophoretic mobility of a highly charged colloidal particle in a solution of general electrolytes, Journal of Colloid and Interface Science, 275 (2004) 665–669. https://doi.org/10.1016/j.jcis.2004.02.078

Oncsik T., Trefalt G., Borkovec M., Szilagyi I., Specific ion effects on particle aggregation induced by monovalent salts within the Hofmeister Series, Langmuir, 31 (2015) 3799–3807. https://doi.org/10.1021/acs.langmuir.5b00225

Oncsik T., Trefalt G., Csendes Z., Szilagyi I., Borkovec M., Aggregation of negatively charged colloidal particles in the presence of multivalent cations, Langmuir, 30 (2014) 733–741. https://doi.org/10.1021/la4046644

Otsuki A., Coupling colloidal forces with yield stress of charged inorganic particle suspension: a review, Electrophoresis, 39 (2018) 690–701. https://doi.org/10.1002/elps.201700314

Overbeek J.T.G., Thermodynamic and kinetic aspects of the electrochemical double layer, Pure and Applied Chemistry, 10 (1965) 359–374. https://doi.org/10.1351/pac196510040359

Park H.M., Electrophoresis of particles with Navier velocity slip, Electrophoresis, 34 (2013) 651–661. https://doi.org/10.1002/elps.201200484

Parsons D.F., Boström M., Maceina T.J., Salis A., Ninham B.W., Why direct or reversed Hofmeister series? Interplay of hydration, non-electrostatic potentials, and ion size, Langmuir, 26 (2010) 3323–3328. https://doi.org/10.1021/la903061h

Parsons D.F., Ninham B.W., Ab initio molar volumes and gaussian radii, The Journal of Physical Chemistry A, 113 (2009) 1141–1150. https://doi.org/10.1021/jp802984b

Peruzzi N., Lo Nostro P., Ninham B.W., Baglioni P., The solvation of anions in propylene carbonate, Journal of Solution Chemistry, 44 (2015) 1224–1239. https://doi.org/10.1007/s10953-015-0335-z

Quezada G., Jeldres R.I., Goñi C., Toledo P.G., Stickland A.D., Scales P.J., Viscoelastic behaviour of flocculated silica sediments in concentrated monovalent chloride salt solutions, Minerals Engineering, 110 (2017) 131–138. https://doi.org/10.1016/j.mineng.2017.04.017

Saka E.E., Güler C., The effects of electrolyte concentration, ion species and pH on the zeta potential and electrokinetic charge density of montmorillonite, Clay Minerals, 41 (2006) 853–861. https://doi.org/10.1180/0009855064140224

Salis A., Pinna M.C., Bilaničová D., Monduzzi M., Lo Nostro P., Ninham B.W., Specific anion effects on glass electrode pH measurements of buffer solutions: bulk and surface phenomena, The Journal of Physical Chemistry B, 110 (2006) 2949–2956. https://doi.org/10.1021/jp0546296

Scales P.J., Johnson S.B., Healy T.W., Kapur P.C., Shear yield stress of partially flocculated colloidal suspensions, AIChE Journal, 44 (1998) 538–544. https://doi.org/10.1002/AIC.690440305

Schneider C., Hanisch M., Wedel B., Jusufi A., Ballauff M., Experimental study of electrostatically stabilized colloidal particles: colloidal stability and charge reversal, Journal of Colloid and Interface Science, 358 (2011) 62–67. https://doi.org/10.1016/J.JCIS.2011.02.039

Schwierz N., Horinek D., Netz R.R., Reversed anionic Hofmeister series: the interplay of surface charge and surface polarity, Langmuir, 26 (2010) 7370–7379. https://doi.org/10.1021/la904397v

Schwierz N., Horinek D., Netz R.R., Anionic and cationic Hofmeister effects on hydrophobic and hydrophilic surfaces, Langmuir, 29 (2013) 2602–2614. https://doi.org/10.1021/la303924e

Schwierz N., Horinek D., Netz R.R., Specific ion binding to carboxylic surface groups and the pH dependence of the Hofmeister series, Langmuir, 31 (2015) 215–225. https://doi.org/10.1021/la503813d

Schwierz N., Horinek D., Sivan U., Netz R.R., Reversed Hofmeister series—The rule rather than the exception, Current Opinion in Colloid & Interface Science, 23 (2016) 10–18. https://doi.org/10.1016/J.COCIS.2016.04.003

Siretanu I., Ebeling D., Andersson M.P., Stipp S.L.S., Philipse A., Stuart M.C., Van Den Ende D., Mugele F., Direct observation of ionic structure at solid-liquid interfaces: a deep look into the Stern Layer, Scientific Reports, 4 (2014) 1–7. https://doi.org/10.1038/srep04956

Sögaard C., Kolman K., Christensson M., Otyakmaz A.B., Abbas Z., Hofmeister effects in the gelling of silica nanoparticles in mixed salt solutions, Colloids and Surfaces A: Physicochemical and Engineering Aspects, 611 (2021) 125872. https://doi.org/10.1016/j.colsurfa.2020.125872

Sthoer A., Hladílková J., Lund M., Tyrode E., Molecular insight into carboxylic acid–alkali metal cations interactions: reversed affinities and ion-pair formation revealed by non-linear optics and simulations, Physical Chemistry Chemical Physics, 21 (2019) 11329–11344. https://doi.org/10.1039/C9CP00398C

Stul M.S., Mortier W.J., The Heterogeneity of the charge density in montmorillonites, Clays and Clay Minerals, 22 (1974) 391–396. https://doi.org/10.1346/CCMN.1974.0220505

Teh E.-J., Leong Y.K., Liu Y., Fourie A.B., Fahey M., Differences in the

rheology and surface chemistry of kaolin clay slurries: the source of the variations, Chemical Engineering Science, 64 (2009) 3817–3825. https://doi.org/10.1016/j.ces.2009.05.015

Tetteh N., Parshotam S., Gibbs J.M., Separating Hofmeister trends in stern and diffuse layers at a charged interface, The Journal of Physical Chemistry Letters, 15 (2024) 9113–9121. https://doi.org/10.1021/ACS.JPCLETT.4C01792

Tian R., Yang G., Li H., Gao X., Liu X., Zhu H., Tang Y., Activation energies of colloidal particle aggregation: towards a quantitative characterization of specific ion effects, Physical Chemistry Chemical Physics, 16 (2014) 8828–8836. https://doi.org/10.1039/C3CP54813A

Tombácz E., Tóth I.Y., Nesztor D., Illés E., Hajdú A., Szekeres M., Vékás L., Adsorption of organic acids on magnetite nanoparticles, pH-dependent colloidal stability and salt tolerance, Colloids and Surfaces A: Physicochemical and Engineering Aspects, 435 (2013) 91–96. https://doi.org/10.1016/j.colsurfa.2013.01.023

Toney M.F., Howard J.N., Richer J., Borges G.L., Gordon J.G., Melroy O.R., Wiesler D.G., Yee D., Sorensen L.B., Voltage-dependent ordering of water molecules at an electrode–electrolyte interface, Nature, 368 (1994) 444–446. https://doi.org/10.1038/368444a0

Vakarelski I.U., Higashitani K., Dynamic features of short-range interaction force and adhesion in solutions, Journal of Colloid and Interface Science, 242 (2001) 110–120. https://doi.org/10.1006/JCIS.2001.7793

Vakarelski I.U., Ishimura K., Higashitani K., Adhesion between silica particle and mica surfaces in water and electrolyte solutions, Journal of Colloid and Interface Science, 227 (2000) 111–118. https://doi.org/10.1006/JCIS.2000.6884

Vereda F., Martín-Molina A., Hidalgo-Alvarez R., Quesada-Pérez M., Specific ion effects on the electrokinetic properties of iron oxide nanoparticles: experiments and simulations, Physical Chemistry Chemical Physics, 17 (2015) 17069–17078. https://doi.org/10.1039/C5CP01011J

Zhang Y., Cremer P.S., The inverse and direct Hofmeister series for lysozyme, Proceedings of the National Academy of Sciences of the United States of America, 106 (2009) 15249–15253. https://doi.org/10.1073/pnas.0907616106

Zhang Y., Furyk S., Bergbreiter D.E., Cremer P.S., Specific ion effects on the water solubility of macromolecules: PNIPAM and the Hofmeister series, Journal of the American Chemical Society, 127 (2005) 14505–14510. https://doi.org/10.1021/ja0546424

Zhao H., On the effect of hydrodynamic slip on the polarization of a non-conducting spherical particle in an alternating electric field, Physics of Fluids, 22 (2010) 1–15. https://doi.org/10.1063/1.3464159

Zhao H., Double-layer polarization of a non-conducting particle in an alternating current field with applications to dielectrophoresis, Electrophoresis, 32 (2011) 2232–2244. https://doi.org/10.1002/ELPS.201100035

Zhou Z., Scales P.J., Boger D. V, Chemical and physical control of the rheology of concentrated metal oxide suspensions, Chemical Engineering Science, 56 (2001) 2901–2920. https://doi.org/10.1016/S0009-2509(00)00473-5

Author's Short Biography

Dr. Tomonori Fukasawa is an Associate Professor at the Graduate School of Advanced Science and Engineering, Hiroshima University. He received his Ph.D. from University of Tsukuba in 2010, followed by postdoctoral position at Kyoto University. His research interests include the kinetics of coagulation, electrophoretic phenomena, rheological properties of particle suspensions, and specific ion effects.